Proceedings of the International Conference on Oxide Materials for Electronic Engineering, May 29–June 2, 2017, Lviv

Optical Properties of $LiNbO_3$-Ag Nanocomposites

I. Bolesta[a], M. Vakiv[b], V. Haiduchok[b], O. Kushnir[a,*], A. Demchuk[a], S. Nastyshyn[a] and R. Gamernyk[c]

[a]Ivan Franko National University of Lviv, Faculty of Electronics and Computer Technologies, Department of Radiophysics and Computer Technologies, 107 Gen. Tarnavskogo Str., 79017 Lviv, Ukraine

[b]Scientific Research Company "Electron–Carat", 202 Stryjska Str., 79031 Lviv, Ukraine

[c]Ivan Franko National University of Lviv, Faculty of Physics, Experimental Physics Department, 8 Kyryla and Mefodiya Str., 79005 Lviv, Ukraine

The article presents the experimental results of the investigation of the absorption spectra and nonlinear refraction of the metal–dielectric nanocomposite that contains the lithium niobate pyroelectric crystal coated with the silver nanofilms on its surface. The atomic force microscopy surface research of these crystals with and without films are also provided. The nanowidth silver films impact on optical spectra and nonlinear refraction of $LiNbO_3$-Ag nanocomposite was analyzed depending on the sign of the side charge of the crystal, that contain nanofilms.

DOI: 10.12693/APhysPolA.133.860

PACS/topics: 68.37.Ps, 71.45.Gm, 81.40.–z, 42.70.Mp

1. Introduction

Lithium niobate $LiNbO_3$ belongs to the class of perovskite crystals ABO_3 and is characterized by high values of pyroelectric, piezoelectric, acousto-optical, electro-optical and nonlinear coefficients, making $LiNbO_3$ one of the main materials for optical devices manufacturing [1]. Currently $LiNbO_3$ is one of the most widely used materials in photonics, based on which acoustic transducers and filters, optical modulators, and converters are produced.

In recent years, the technologies of linear and nonlinear microstructure on the surface of $LiNbO_3$ are rapidly developing, which leads to the construction of photonic crystals [2, 3].

The study of plasmon responses in metal nanoparticles deposited on the surface of the dielectric matrix indicates their significant impact on non-linear and linear susceptibility matrix [4, 5]. Therefore, we can expect that construction of metallic nanoparticles on the $LiNbO_3$ surface also leads to changes in linear and nonlinear properties of the metal–dielectric nanocomposites, which might be useful to extend its practical application.

In this paper the morphology of silver nanoparticles deposited on the surface of the monocrystalline $LiNbO_3$ and its impact on the linear and nonlinear optical response of the metal–dielectric nanocomposite are studied.

2. Experimental

Silver films were obtained from magnetron sputtering in vacuum on the installation for combined sputtering COM-TH2-SP2-ION (TORR, USA). The films were sputtered onto $16 \times 8 \times 0.8$ mm^3 substrates. The substrates were fabricated from monocrystalline lithium niobate, with the crystallographic axis Z directed perpendicularly to the substrate plane.

The thickness of the silver films was varied in the range of 1–4 nm, the film sputtering was performed at a speed of 0.7 Å/s, the substrate temperature was equal to 50 °C.

The topology of the surface was investigated with the use of an atomic force microscope (AFM) NT-MDTSolverPro 47 and was registered in a semicontact regime, by applying an NSG 10, probe with a tip radius of about ≈ 10 nm. Numerical parameters for elements of the film structure were obtained by the combination of methods surface topology cut algorithm with automatically height select and the watershed method [6]. This procedure allowed us to distinguish the particle boundaries on the image, determine the particle shape, and find the geometrical parameters. In order to enhance the reliability of the results, the data obtained for the surface topology at various film sites were averaged over the ensemble.

The transmission and reflection spectra were measured using the double-beam spectrophotometer Shimadzu UV-3600 in 300–1600 nm interval with a step of 1.0 nm and a spectral slit bandwidth of 2.0 nm. A halogen lamp served as a light source, a photomultiplier was used as a detector in an interval of 300–960 nm, and an InGaAs photodiode played the role of a sensor in the wavelength interval above 960 nm. The reflection spectra were measured with the use of an ASR-3105 attachment with the complete specular reflection at an incidence angle of 5°. The absorption spectra were calculated based on the transmission and reflection spectra values.

For research of nonlinear optical properties of $LiNbO_3$ with Ag film we used traditional one beam Z-scan technique developed by Sheik-Bahae et al. [7]. Measurements were performed at the room temperature using the sec-

*corresponding author; e-mail: alex.kuschnir@gmail.com

ond harmonic continuous emission of the neodymium laser with diode buildup that operates at a wavelength of 532 nm. The output power of the laser beam was 45 mW. Parameters of the focused laser beam meet the essential requirements of Z-scan experiment: $2\omega_0 = 22.3$ μm (ω_0 — Gaussian beam radius in the focus); $b = \frac{n\pi\omega_0}{\lambda} = 1.197$ mm (b — diffraction length in the Rayleigh band), the power density of the laser beam in the focus $I_0 = 1.04 \times 10^4$ W/cm^2.

Z-scan experiment allows us to calculate nonlinear refractive index n_2, included in known expression for the total refractive index $n = n_0 + n_2|E|^2$, where n_0 — linear refractive index, E — the amplitude of the electric field intensity of the laser radiation. Nonlinear refractive index n_2 on normalized Z-scan spectra conducted by the formulae [8]:

$$n_2 = \frac{\Delta\Phi_0}{kL_{eff}I_0}, \tag{1}$$

where $\Delta\Phi_0$ — nonlinear phase distortion, $k = \frac{2\pi}{\lambda}$ – wave vector, I_0 — the maximum intensity of the laser in focus, L_{eff} — effective thickness of the sample:

$$L_{eff} = \frac{1 - e^{-\alpha L}}{\alpha}, \tag{2}$$

where α — linear absorption coefficient at wavelength of 532 nm, L — thickness of the sample.

Nonlinear phase distortion $\Delta\Phi_0$ empirically associated with a change in normalized transmittance $\Delta T_Z = T_{+Z} - T_{-Z}$, obtained from the experimental Z-scan spectrum

$$|\Delta\Phi_0| \cong \frac{\Delta T_{pv}}{0.406(1-S)^{0.27}}, \tag{3}$$

where S — transmission aperture without sample, ΔT_Z — the difference of the transmission maxima T in case of positive (T_{+z}) and negative (T_{-z}) coordinates Z. In our experiment with a closed diaphragm S is equal to 0.07 of the incident light aperture intensity.

3. Results and discussion

The absorption spectra of Ag films, sputtered on the positively charged surface of the $LiNbO_3$, contain band with maximum shifted from 520 to 610 nm depending on growing mass film thickness (Fig. 1a).

A comparison of the obtained data with the spectra of Ag films sputtered on glass substrates below the percolation threshold [9] allows to associate the band in the $LiNbO_3$-Ag with the surface plasmon resonance of silver nanoparticles formed on the surface of $LiNbO_3$ after sputtering. However, the spectral position of the band is shifted significantly to the long-wavelength region compared with the spectra of Ag films on glass substrates [9]. To confirm this conclusion, the spectra were obtained in the one process cycle for Ag films on the glass substrate and on positively and negatively charged $LiNbO_3$ surfaces (Fig. 1b).

The position of the peak of plasmon absorption of silver nanoparticles on a glass substrate is at 532 nm, while for $LiNbO_3$ substrates the peak position equals to 564 nm

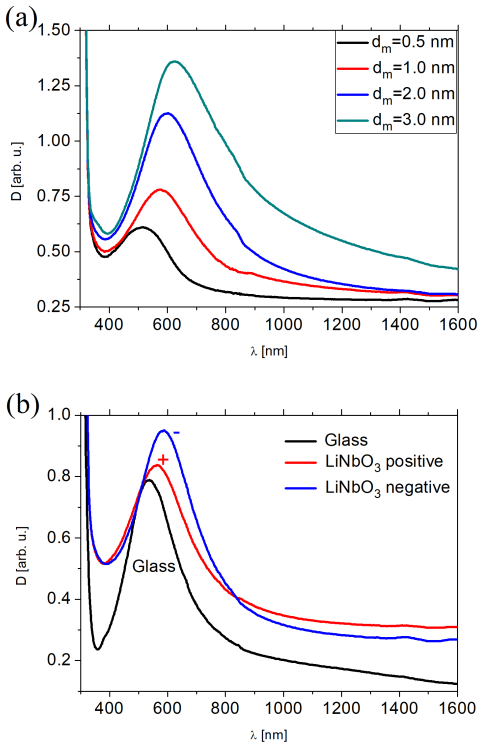

Fig. 1. Experimental absorption spectra of silver films sputtered on the positively charged surface of $LiNbO_3$ with different mass thickness (a) (shown in the figure) and absorption spectra of silver nanofilm with 1 nm mass thickness deposited on a glass, positively and negatively charged crystal surface.

and 587 nm for positively and negatively charged surfaces, respectively.

The mass thickness of the Ag films, sputtered in one process cycle on the $LiNbO_3$ and glass substrates is the same, therefore the difference in the position of the maxima can be caused by several factors. The one factor is higher refractive index of lithium niobate in comparison to glass, which increases the impact of the effective dielectric constant around the metal particles. However, considering that the metal nanoparticles contact not only with the substrate, but also with the air, the change in effective dielectric constant is insufficient for such a shift.

Another important factor that affects the position of the plasmon resonance band is a shape of particles generated on glass and $LiNbO_3$.

Figure 2a presents AFM surface topology of pure $LiNbO_3$. The surface roughness for this image is $RMS_{LNO} = 2.57$ nm. Figure 2b presents the AFM topology of the Ag film surface on the $LiNbO_3$ substrate in the same scale. The roughness of this surface is $RMS_{AG} = 3.52$ nm. In another scale, the presence of individual silver nanoparticles on the surface becomes obvious (Fig. 2c). Digital processing with watershed method [6] allowed us to obtain the numeric properties of the individual silver nanoparticles. The received distri-

butions are shown in Fig. 3. From comparison of distributions by equivalent radii (Fig. 3a) and height (Fig. 3b) we infer the form of average nanoparticles, that formed during the silver film with mass thickness $d_m = 1$ nm sputtered on the $LiNbO_3$ surface. The average particles have the oblate spheroid form (disks) with the mean radius $r = 7$ nm and height $h = 1.2$ nm. Then the relation r/h can be considered as the ratio of the main axes $a/c \approx 5.8$ of oblate spheroid.

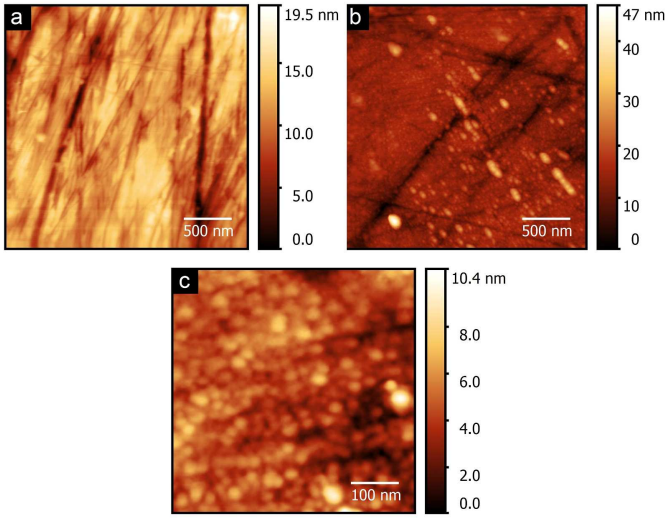

Fig. 2. AFM image of the surface morphology of lithium niobate (a) and Ag film with 1 nm mass thickness deposited on the surface of $LiNbO_3$ on the same scale (b) and at higher scale (c) to identify silver nanoparticles.

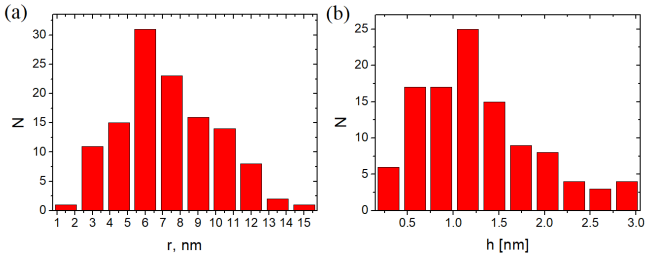

Fig. 3. The distribution of silver nanoparticles on radius (a) and height (b), derived from the AFM data.

For similar reasons and from the data presented by us in [9], the ratio of the main axes for the films with a mass thickness about 1 nm on the glass $a/c \approx 1.4$.

Considering the AFM data we can assume that spheroidal form of Ag nanoparticles on the $LiNbO_3$ surface determines the existence of at least two plasmon modes: longitudinal and transverse. Mode, associated with longitudinal oscillations of charge carriers, is shifted to the long-wavelength region in comparison with the spherical particle. Thus, in the spectrum of $LiNbO_3$-Ag only longitudinal oscillation mode can be observed. It should be noted that the surface charge of the lithium niobate can shift the charge carriers in the nanoparticles, which also affects the frequency of plasmon resonance in them [10], resulting in the different spectral position of the absorption maxima for nanofilms, deposited on crystal surface with different signs of pyroelectric charge. It should also be noted that the maximum of the plasmon absorption for silver film deposited on the negatively charged side shifted into the long-wavelength region for this reason.

Figure 4 shows the Z-scan spectra of $LiNbO_3$ crystals with the silver film of 1 nm mass thickness deposited to the negatively charged crystal surface (Fig. 4a) and positively charged crystal surface (Fig. 4b). The label 01 near the curves in the figures corresponds to the direction of light propagation through the film firstly and further through the crystal (front film), and the label 02 near the curves — through film behind the crystal along the light. It should be noted that the nonlinear refraction in all cases is positive (it shows the direction of the scanning curve in the beam focus point). To calculate nonlinear refractive, we take the resulted values of difference ΔT. In the case of a film on the negative surface "-" $\Delta T = 0.1412$ (curve 01) and $\Delta T = 0.0912$ (curve 02). For the films on the positive surface "+" $\Delta T = 0.0591$ (curve 01) and $\Delta T = 0.084$ (curve 02). To analyze the influence of crystal surface on the value of nonlinear refraction will use the value ΔT, because the thickness of the effective layer is not evident. The difference between the surface roughness of pure lithium niobate and the surface with 1 nm mass thickness silver film is, as expected, ≈ 1 nm, but the difference in height and, therefore, the position of silver nanoparticles on the axis Z, is more than 40 nm. This causes the ambiguity in the choice of the active layer thickness value, because a value is significantly greater than the geometric dimensions of silver nanoparticles.

Analyzing the impact of metal nanoparticles on the nonlinear properties of $LiNbO_3$-Ag nanocomposite, we should take into account that the optical nonlinearity is caused by the two effects. The thermal effect occurs through the transfer of heat, that appears in the nanoparticle surface during the incidence light oscillations, from the surface of metallic nanoparticles to the surface of the niobate crystal. Electro-optical effect is caused by polarization of the strong surface plasmon resonance and the heterogeneous placement of nanoparticles on the surface. However, the electro-optical effect emerged as a result of the crystal surface pyroelectric charge.

Based on the experimental results we can say that coating the lithium niobate surface with the silver nanofilms has a significant effect on the nonlinear refraction of $LiNbO_3$-Ag nanocomposite, especially for light transmission through the metal film firstly. Particularly interesting thing is the experimental fact that silver nanofilms have different effects on the nonlinear refraction of $LiNbO_3$-Ag composite depending on the sign of the surface charge. While the nanofilms are sputtered

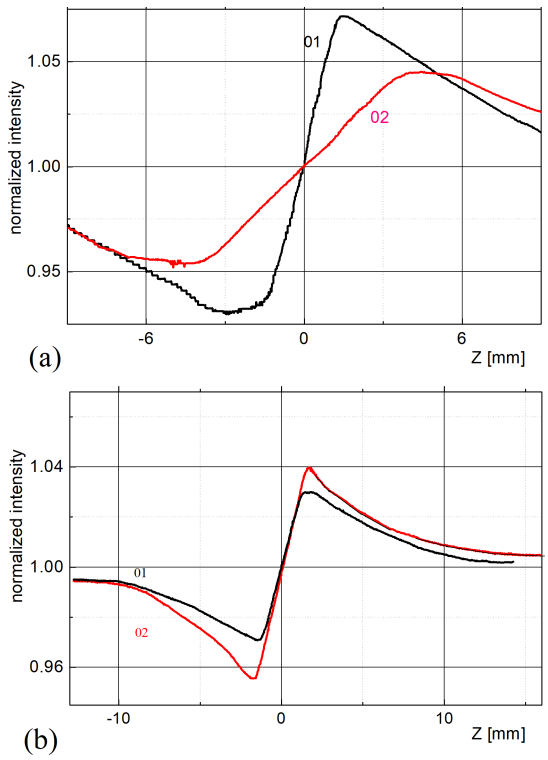

Fig. 4. *Z*-scan spectra of the silver nanofilms, sputtered on the negatively charged (a) and the positively charged (b) surface of $LiNbO_3$ crystal. Curve 01 corresponds to the light propagation in the "film–crystal" direction, 02 — "crystal–film".

on the negatively charged crystal surface the nonlinearity increases, and on the positive charged surface — on the contrary, decreases.

4. Conclusions

To summarize, while sputtering the silver nanofilms on the surface of a lithium niobate crystal the disk-shaped nanoparticles are formed, in which the surface plasmon resonance appears as the response to the incident light, this resonance manifests in the absorption spectra band. With the increasing mass thickness of the nanofilms maximum peak of the resonance shifts to long-wavelength region. The position of the maximum also depends on the crystal surface charge sign: plasmon, the absorption peak position shifted to long-wavelength region when Ag films are sputtered on the negatively charged side of the $LiNbO_3$ crystal. A similar impact of nanofilm on the nonlinear refraction of nanocomposite is also detected. When the film is sputtered on the negatively charged side of the $LiNbO_3$ crystal, nonlinear refraction increases, particularly while light propagates in the "film–crystal" direction, whereas when the film is sputtered on the positively charged side — on the contrary, nonlinear refraction decreases. This effect can be used to determine a charge sign of lithium niobate surface in the relatively simple way.

References

[1] R.S. Weis, T.K. Gaylord, *Appl. Phys. A* **37**, 191 (1985).

[2] M. Manzo, F. Laurell, V. Pasiskevicius, K. Gallo, *Appl. Phys. Lett.* **98**, 122910 (2011).

[3] M. Manzo, F. Laurell, V. Pasiskevicius, K. Gallo, *Opt. Mater. Expr.* **1**, 365 (2011).

[4] V.T. Adamiv, I.M. Bolesta, Ya.V. Burak, R.V. Gamernyk, I.D. Karbovnyk, I.I. Kolych, M.G. Kovalchuk, O.O. Kushnir, M.V. Periv, I.M. Teslyuk, *Physica B* **449**, 31 (2014).

[5] I.M. Bolesta, O.O. Kushnir, I.I. Kolych, I.I. Syvorotka, V.T. Adamiv, Ya.V. Burak, I.M. Teslyuk, *Adv. Sci. Eng. Med.* **6**, 1 (2014).

[6] R.C. Gonzalez, R.E. Woods, *Digital Image Processing*, 3rd ed., Pearson, London 2008.

[7] M. Sheik-Bahae, A.A. Said, T.H. Wei, D.J. Hagan, E.W. Van Stryland, *J. Quant. Electron.* **26**, 760 (1990).

[8] G.V. Arnold, *J. Appl. Phys.* **46**, 4466 (1975).

[9] I.M. Bolesta, O.O. Kushnir, *Ukr. J. Phys. Opt.* **13**, 165 (2012).

[10] I.M. Bolesta, M.M. Vakiv, V.G. Haiduchok, A.A. Kushnir, *Ukr. J. Phys.* **62**, 39 (2017).